



### **Science Arts & Métiers (SAM)**

is an open access repository that collects the work of Arts et Métiers Institute of Technology researchers and makes it freely available over the web where possible.

This is an author-deposited version published in: <https://sam.ensam.eu>  
Handle ID: <http://hdl.handle.net/10985/9220>

#### **To cite this version :**

Nazih MECHBAL, Euripedes NOBREGA - Spatial H Approach to Damage Tolerant Active Control  
- Structural Control and Health Monitoring - Vol. XXX, n°XXX, p.27 - 2015

Any correspondence concerning this service should be sent to the repository

Administrator : [scienceouverte@ensam.eu](mailto:scienceouverte@ensam.eu)



# Spatial $H_\infty$ Approach to Damage Tolerant Active Control

Nazih Mechbal<sup>1\*</sup> and Eurípedes G. O. Nóbrega<sup>2</sup>

<sup>1</sup> *Processes and Engineering in Mechanics and Materials Laboratory, Arts et Métiers ParisTech, Paris, France*

<sup>2</sup> *Department of Computational Mechanics, UNICAMP, Campinas, SP, Brasil*

## ABSTRACT

Damage tolerant active control is a new research area targeting to adapt fault tolerant control methods to mechanical structures submitted to damage. Active vibration control is a mature engineering area, using modern control methods to address structural issues that may result from excessive vibration. However, the subject of structural vibration control under damage represents a novel subject in the literature. There are some difficulties to adapt regular controller designs to active control, which may not result in good performance even for healthy structures. Fault detection and diagnosing research has conducted to development of the fault tolerant control area, whose methods are equally hard to translate to damaged structure control. Spatial active vibration control encompasses some techniques that present important features to structure control, however this is not necessarily true in the general control design area, where spatial constraints are normally not involved. We propose in this paper an investigation of these spatial techniques, applied to structural damage control. Several new strategies for vibration control are presented and analyzed, aiming to attain specific objectives in damage control of mechanical structures. Finite element models are developed for a case study structure, considering healthy and three different damage conditions, which are used to design controllers, adopting an approach based on a  $H_\infty$  spatial norm, and according to some of the proposed strategies. Discussion of the achieved results contributes to clarify the main concepts related to this new research area, and controller performance analysis permit to foresee successful real case application of the techniques here described.

**KEY WORDS:** Damage Tolerant Active Control, Spatial  $H_\infty$  Control, Fault Tolerant Control, Structural Health Monitoring, Active Vibration Control, Piezoelectric, Smart Structures, Finite elements.

---

## 1 INTRODUCTION

Development of new technologies and materials, aiming to extend the operative life of mechanical structures and increase the level of safety standards, constitute a modern challenge that calls for the use of advanced tools, methods and procedures. New generations of mechanical structures based on smart materials possess the ability to change their physical properties in response to specific stimulus. Embedding smartness to structures improves its intrinsic or extrinsic characteristics and entails innovations beyond the ingenious design of final products. It also brings significant impact on processes and systems adopting the new structures. For example, smart composites can present the ability to monitor its structural health and therefore to guarantee better control of its passive, active or adaptive functions. Smart structure development in general opens new fascinating frontiers for applied research and product engineering.

---

<sup>1\*</sup> Corresponding author, PIMM (UMR – CNRS 8006), Arts et Métiers ParisTech (ENSAM), Paris, France. E-mail: [nazih.mechbal@ensam.eu](mailto:nazih.mechbal@ensam.eu)

<sup>2</sup> E-mail: [egon@fem.unicamp.br](mailto:egon@fem.unicamp.br)

Recently, the concepts of Damage Tolerant Active Control (DTAC) were proposed [1]. DTAC systems represent a new research area that has intersections with both Fault Tolerant Control (FTC) and active control of vibration areas. DTAC systems' framework is based on Structural Health Monitoring (SHM), in the same way that most FTC methods rely on Fault Detection and Diagnosis (FDD) systems, to provide feedback data used to achieve the performance goals of the controller [2]. Intense research activity in the last decades brought to maturity several methods of the aforementioned areas. This effort represents the application of multidisciplinary monitoring methods to assess complex systems of modern engineering, seeking essentially safe operation and useful life extension for these systems, generally based on evaluation of their operational status, and eventually applying control methods to ensure the required performance. DTAC systems therefore comes to use a wide multidisciplinary context, applying knowledge from different fields, such as mechanical structures modeling, signal processing, instrumentation, fracture mechanics, modal analysis and artificial intelligence, among others.

SHM methods provide fault detection and diagnosis of the state of a mechanical structure [3] [4] [5] [6] [7]. Such methods have been developed at various engineering sectors, especially air or land vehicles [8] [9] and civil structures [10]. SHM is now considered the key technology to pave the transition from traditional schedule-driven to condition-based maintenance [11].

Active control of mechanical structure vibrations has evolved significantly in the last two decades [12] [13] [14]. A known example of successful application of these methods is the response control of buildings to vibrations caused by winds or earthquakes [15] [16]. Several other problems have been treated in the literature [17] [18], and an increasing number of applications may become common in the near future, following the trend of lighter structures.

Fault detection techniques associated to control methods have conducted to the development of the FTC area, beginning with the case of a robust controller that is designed to encompass some previously conceived faults. This is known as *passive* FTC, despite the fact that a controller is involved, because the controller is not expected to change due to the occurrence of a fault. Two main classes of *active* FTC methods, *when the controller changes*, may be identified: the reconfiguration of the controller in face of faulty conditions, in order to maintain adequate performance; or the fault accommodation through switching the controller to another one previously designed [19] [20] [21]. However, simple application of these active FTC methods to damaged structures brings new challenges, and consequent specific solutions, thereby generating the new area of DTAC. To the better knowledge of the authors, there are very few publications applying active reconfigurable or switching control of vibration techniques to damaged structures. Attempts to design control architectures that take fatigue into account, in order to prevent from potential damages, have been proposed recently in [22] and [23].

Smart structures include in general embedded sensors, actuators and eventually processors, enabling them to diagnose and react to abnormal states, and thus minimizing the effects of a possible damage. Including embedded digital processors, smart structure capabilities may integrate a high level of computational intelligence. New methods and procedures are necessary, conducting to automatic analysis, diagnosis and damage control processes. The range of embedded techniques to monitor and control mechanical structures now can adopt a large amount of transducers, routines for the detection of faults, its diagnosis and prognosis, and also the reconfiguration of the active control algorithms in response to a damage, be it a permanent change or a specific response facing an emergency or harsh situation.

Pursuing DTAC goal to control damaged smart structure vibrations, two different controller

objectives may be adopted: vibration suppression in the whole structure or only in some specific parts. In this paper, an approach to DTAC system design, based on spatial  $H_\infty$  norm, is presented, aiming to maintain acceptable performance for a possibly damaged controlled structure. Active vibration control of structures is basically concerned with spatially distributed systems. These system models are governed by partial differential equations that can be discretized using a modal analysis procedure, which leads to mode shapes that describe the spatial characteristics of the structure. In the case of irregular geometries and non-trivial boundary conditions, analytical solutions are not available to generate this type of model. Finite Element (FE) and system identification methods are often used to represent spatially distributed models. Numerical simulations provide the ability to understand the relative effects of property changes in great detail, such as brought by damage, and are thus quite fundamental for design. In this work, FE models, for healthy and damaged smart structures, are used to design spatial controllers intended to manage vibration suppression in the presence of structural damages.

The common approach to active vibration control design is to assume an input disturbance in one or more specific positions, with authority to locally excite dominant modes. In this case, and especially if a damage is present, one needs to adjust the controller for each considered vibration mode, in order to not increase unexpected vibration modes at some structure regions (damaged or not). Furthermore, it is common to have some specific position to measure the vibration to be controlled, often in a collocated configuration of inputs and outputs. Applying a  $H_\infty$  based approach, which is currently the preferred design method for active vibration control, early work of the authors [24] has investigated a combined scheme allowing vibration rejection and sensor faults detection on smart structures. As in these approaches, one use only specific points for input and output, it does not adequately take into account the spatial restrictions of the structure. This opens the way to spatial norm definitions and respective controller design methods [25].

To control (healthy) structures, some early works introduced the application of spatial norms [26] [27]. The authors proposed to use spatially distributed models instead of these mentioned point-by-point framework or, as generally called, pointwise models. These norms have been employed to elaborate collocated optimal  $H_2$  and  $H_\infty$  spatial controllers that ensure vibration reduction over entire structures in a spatially average sense. This is done by employing the spatial information embedded within the models of structures that result from modal analysis. Robustness of collocated controllers have been investigated and implemented effectively on real structures using piezoelectric transducers (PZT) by [28] [29] and [30]. The improved performance obtained using spatial approach to control healthy structure vibration is well established now [31] [32].

The objective of this paper is to further explore issues in vibration analysis for smart structure testing and control, considering the occurrence of damage. It presents a spatial approach to perform DTAC on damaged smart structures. We propose to investigate  $H_\infty$  spatial control applied to damaged structures with non-collocated PZT sensors and actuators, under some strategic treatment of DTAC goals. Comparing collocated and non-collocated configuration, the last one present restricted stability performances and do not have necessarily the same number of inputs and outputs [13] [33]. Structures always present flexibility between the actuator position and the region where the vibration must be attenuated, which entails the collocated concept only for theoretical applications. Composite smart structures, constructed with the active elements embedded in non-isotropic composite layers, are clearly the non-collocated case. Discussions of FE simulated results are here presented, adopting the spatial approach and new control strategies, which are applied to a case study smart structure.

The outline of the rest of the paper is the following: in Section 2 DTAC different strategies and respective controller architectures, which are going to be explored in the examples, are presented; in Section 3, the Finite Elements models used in the simulations are given, including details about transducers and damages representations; in Section 4, the mathematical model approach for spatial norm based controller design is presented; in Section 5, simulated results for a cantilevered structure is developed, including a spatial robust controller and damage effects; in Section 6, application of some DTAC configurations and strategies are analyzed; a discussion of the results is presented in Section 7 and final remarks and future perspective are drawn in the last section.

## 2 STRUCTURES AND DAMAGE CONTROL

DTAC systems mean essentially active control of mechanical vibrations of structures aiming to maintain an adequate performance under the possibility of structural damage. Applications demand a network of transducers to produce measurement data to feedback the control loop, but also to feed specialized modules implementing structural integrity analysis techniques, in order to guarantee that the DTAC controller attains its goals. Ergo, the structure has to be smart to embed a DTAC system. A brief insight of smart structure constitution is given in the sequence.

### 2.1 *Smart functions in structures*

Advanced structures with improved self-capabilities have been intensively studied over the last four decades [34]. A smart structure needs the ability to respond to internal changes and also to environmental conditions. It means that built-in sensors and actuators are necessary, to monitor and diagnose these changes. Smart structures emulate some characteristics of a biological system as sensing, actuation, adaptability and self-repair. Development of smart structures is fuelled by the on-going technological progress and evolution of performance demands.

Different materials can be used on smart structures to act and sense. Among possible current transducers, piezoelectric materials are those widely used, due to their adaptable properties. Because piezoelectric elements can be used for mechanical to electrical transduction and vice-versa, they can be adopted as sensors and/or actuators, which makes it easier to integrate the smart functions to the structure. Commonly used piezoelectric materials are semicrystalline polymer film PVDF (polyvinylidene fluoride), and PZT ceramic (lead zirconate titanate).

Nowadays, and particularly in aeronautical industry, composite materials are increasingly used due to their strength properties. Because of its multilayer structure, they are suitable to host smart materials. Indeed, embedded sensors and actuators could be easily incorporated into the composite as a smart layer, during or even after the manufacturing phase of the composite panels.

Therefore, based on the adopted objectives to perform structural active control, different strategies may be considered, depending if the structure is in a healthy condition or if damage was detected. The respective framework is presented in Fig. 1, where the strategies depend if the structure has an identified damage or not. If the structure is a healthy one, there are two strategies:

- Strictly tolerant active control;
- Preventive active control;

If damage is identified there are two other strategies to be applied:

- Evolving damage active control;
- Adaptive tolerant active control.

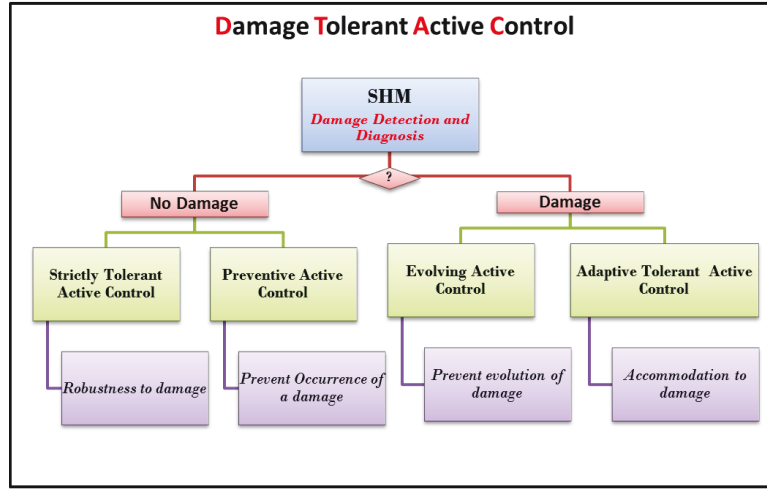


**Fig. 1:** Structural active controllers under possible damage

It is also possible that a DTAC system may combine these strategies, but this will not be treated here. A description of the four above possibilities is presented in the following.

A robust control is the first step to face damage that may occur in the future to the structure. The basic objective here is to design an active controller that rejects specifically some considered modes. Indeed, targeting the vibration level of the most damaging mode of some structures, subjected to known severe stress conditions, can enhance its longevity. As an example, one can refer to [23], where the authors proposed an active logic for the damage reduction of printed circuit boards by means of piezoelectric actuators and sensors. A strictly tolerant active controller (STAC) is the strategy to be used to design a controller robust enough to guarantee a minimal acceptable performance even if damage occurs. The resultant controller is fixed, meaning that it will not necessarily respond to parameter changing in the structure, beyond its already included robustness capacity. The applicability of this strategy is limited, and basically depends on the predictability of future damages and its respective severity. Nevertheless, the compromise between robustness and performance may conduct to a poor controller behavior for a not damaged structure.

A preventive active control (PAC) is the strategy to be used when the controller is designed to avoid or retard the occurrence of damage. An example of this strategy is presented by [22], where a cost function includes an expression that take into account material fatigue, which is then minimized in the controller design process. The main goal here is to guarantee a longer structure life based on the use of a PAC system. Again the controller does not change if damage is detected.

If damage is detected and identified, an evolving damage active controller (EDAC) is the strategy to design a controller to protect the structure. The main goal is to minimize the vibration energy flow to the damaged region in order to avoid the damage evolution. It may be typically used in a smart structural repair, which now can monitor and control the extent of damage [35].

The last strategy general approach is to accommodate a detected damage and at the same time maintain an adequate level of performance. Consider a smart structure with a network of sensors and actuators including an SHM module and an active vibration controller. When damage is detected, the controller shall be adapted to face the new structural condition. This is the adaptive tolerant active control (ATAC) novel strategy, mainly addressed in this paper. Some different system configurations are examined briefly in the next paragraphs.

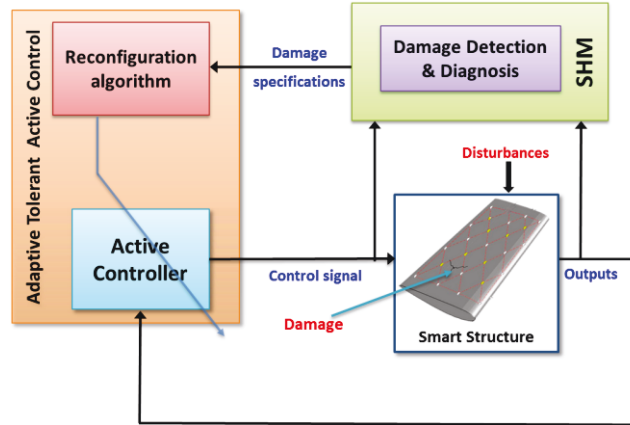


**Fig. 2:** DTAC scheme in a reconfigurable design

The first and simplest ATAC configuration is to depend on a human interaction to design a new controller. An existing SHM module must provide enough information so that an engineer may be able to design a new controller to guarantee the required performance. Evidently, this may not be applicable for emergency situations, where a rapid response is necessary. In this case, an automatic reconfiguration of the controller is indicated. The automatic reconfiguration mechanism and the FDD module interaction is the subject of a future publication, demanding its proper space to detail the reconfiguration method.

To be able to perform online the reconfiguration, and ensure a fast response of the controller to a sudden change of structural behavior, the FTC main configurations [21] [36] may be adopted. The main difference between FTC and DTAC are the specific methods to be adopted for controller design, which must take into account spatial restrictions necessary to provide effective control of structural vibrations. The FTC typical framework is depicted for DTAC in Fig. 2.

Comparing the block diagram seen in Fig. 2 with a regular feedback controller diagram, it may be noticed the introduction of two new blocks, respectively SHM and ATAC, which includes the reconfiguration algorithm and the active controller. The SHM module must provide information to the reconfiguration algorithm to be able to change the active controller online. Signals that come from the SHM block may be a residue vector, generated by recent input and output signal measurements, weighed against a validated signature of the healthy structure. However, for DTAC systems, more information may be necessary, such as severity and localization of damage, or other data required by the reconfiguration algorithm, for example pole deviations due to damage, or semantic information for an artificial intelligence based reconfiguration.

Considering that even if this controller reconfiguration mechanism should respond as fast as possible, eventually the implicit time delay may bring some difficulty to its application when a really fast response is necessary, for example, in the case of serious and sudden aircraft damage. New elaborations over this scheme may avoid catastrophic consequences of time delay, but they will be treated in future publications.

### 3 ACTIVE SMART STRUCTURE AND FE MODEL

The FE models of the cantilevered structure represented in Fig. 3, equipped with non-collocated and surface-mounted piezoelectric patches, are developed in the next sections. Models of the healthy structure, including representation of the piezoelectric patches, are used to assess the

undamaged performance. Developed models of the structural damages are also based on patches, and used to simulate the closed-loop behaviour under the action of different DTAC controllers.

### 3.1 Adopted composite smart structure

We adopt in this study an active cantilevered laminate plate in a horizontal position, according to dimensions ( $920 \times 192 \times 1.2 \text{ mm}$ ) and elements in Fig. 3, which is modeled with the complete six degree-of-freedom (DOF) at each node in a dense FE grid, in order to have the complete dynamics represented as realistic as possible. The structure consists in four epoxy/carbon layers with orientation angle  $[0^\circ/-45^\circ/+45^\circ/0^\circ]$ . The actuators are circular PZT patches from NOLIAC<sup>®</sup> and sensors are flexible macro fiber ceramic (MFC), from Smart Materials<sup>®</sup>. Material properties for the layers, piezoelectric elements and respective glue are given in the Appendix.

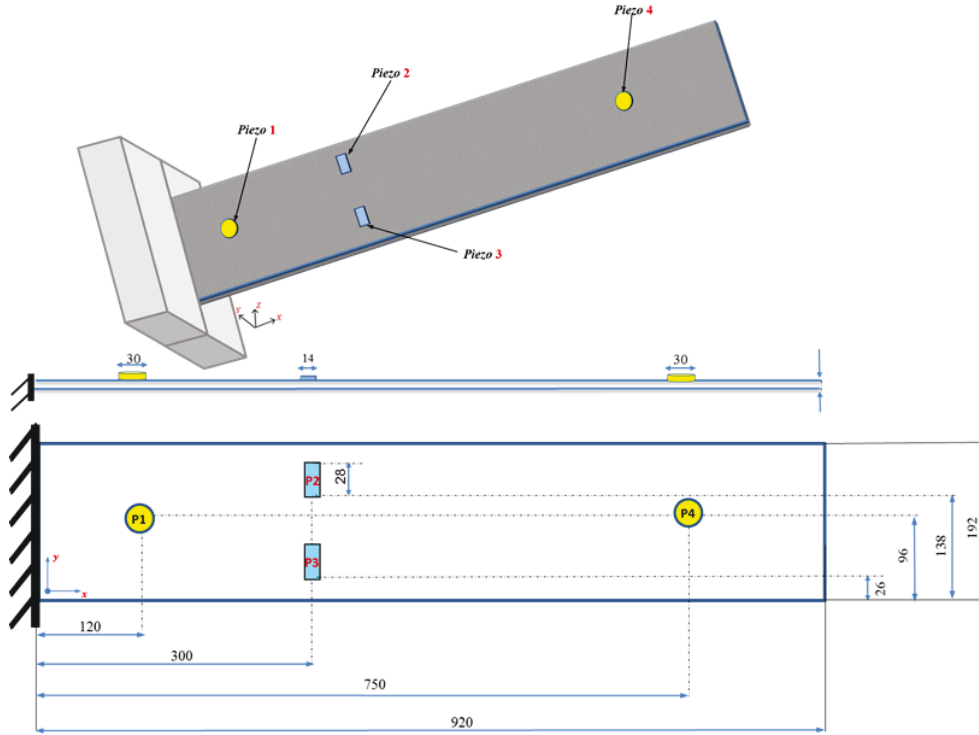


**Fig. 3:** Adopted composite structure with active elements

### 3.2 Piezoelectric transducers

A key challenge is to achieve a good validated model for the piezoelectric patches, and their interactions with the composite structure. Thereby, we tested and identified the mechanical properties of composite specimens, for the transducers' parameters in the FE models [9]. Accordingly, piezoelectric patches have been glued on these specimens and electromechanical measurements have been performed for correlation studies [9].

The smart structure FE models developed in this work use the Structural Dynamics Toolbox for MATLAB<sup>®</sup> (SDT) [37], based on piezoelectric Mindlin shells, taking into account the viscoelasticity of the composite core, the glue, and the piezoelectric coupling equations. Electrical degrees of freedom (DOF) are included in addition to the nodal displacement [38].



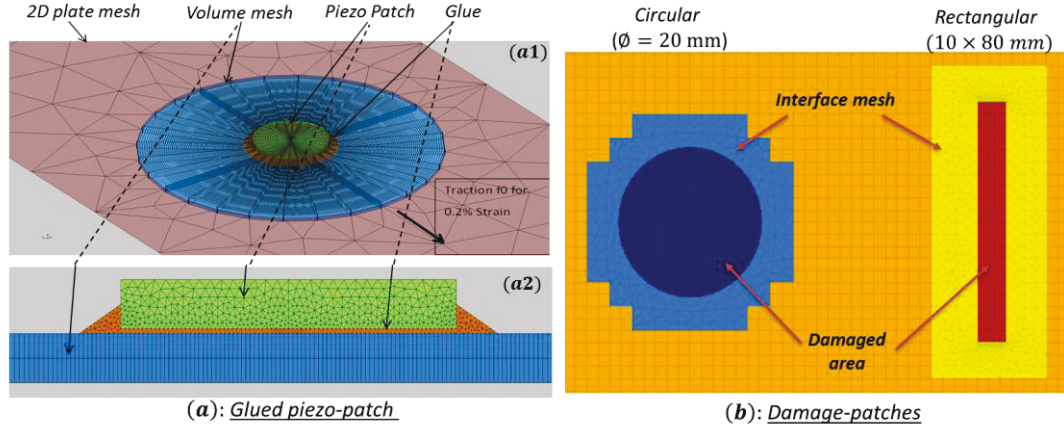


**Fig. 4:** (a) Geometric representation of the glued piezo-patch : (a1) Top view; (a2) zoom with a side view. (b) Example of damage-patches.

For piezoelectric shell elements, electrical DOFs correspond to the difference of potential on the electrodes while the corresponding load is the electrical charge. For volume elements, one defines multiple point constraints to enforce equal potential on nodes linked by a single electrode and sets one of the electrodes to zero potential. To represent sensors, the configuration corresponds to cases where the voltage remains very small and an electrical charge is generated basically due to mechanical deformations. For the actuator configuration the electrical charge corresponds to the resulting force associated with the voltage, applied through a voltage driven amplifier [39].

Considering dynamic measurements, one expects that the first in plane mode of the patch, due to Poisson's effect, will generate compression through the thickness and thus a charge distribution on the surface [40]. To bypass the need to compute all modes in the frequency range of interest, the proposition is to compute the direct frequency response on a given range and to use the resulting shapes to build a Ritz basis. Further details on this method may be found in [41], but the approach guarantees good results at the retained frequencies and is deemed most efficient for the considered applications.

### 3.3 FE patches modeling

Referencing to Fig. 4a, to account for material properties, one considers a volume mesh distinguishing an orthotropic base plate (shown in blue), a glue layer (EPO-TEK) assumed to be an isotropic elastic material, (in orange), and a transversely isotropic piezoelectric material (shown in green). The electrodes are placed on the circular surfaces and polarization is in the direction normal to the surface.

Based on a Stiffness Reduction Method (SRM) [42], a parametrical damage is introduced through the parameter  $\gamma$ . Indeed, in SHM context, a common and simple way of modeling damage is to incorporate a stiffness loss in the region of the damage by modifying the respective materials properties. We represent this change using the vector  $P_{mat}$  (Young's modulus, shear modulus, density etc.) to the product  $\gamma P_{mat}$  with  $\gamma \leq 1$  [42]. Therefore, to introduce this damage, an automatic approach has been developed using SDT software where a damage-patch is generated with a specific mesh. The dimension and the material properties of this damage-patch could then be changed and adjusted. The introduction of this patch before changing its properties

does not alter the modal properties of the structure. Moreover, nodes inside this damage-patch could be removed to create crack damages. It is possible to see in Fig. 4b two examples of this automatic generated approach to represent damage in FE models. Notice also that there is a mesh for the structure, a different one for the damage boundaries and a third for the damage itself.

## 4 SPATIAL NORM-BASED CONTROL DESIGN

An active vibration control methodology based on a spatial  $H_\infty$  norm definition [30] has been studied in the last two decades, starting from the initial work of [26]. This approach may be very useful to DTAC systems, and is explored further in this paper. It must be emphasized that application of these concepts to damage control is probably unique to DTAC, representing a control methodology that may not be used by a regular FTC system. The idea is to control the vibration in predefined *regions of the structure*, instead of having pointwise controllers, *i.e.* a norm minimization at *specific points* where the structure has performance indicators or sensors.

In pointwise active control, the controller is designed based only on the information of some positions along the structure [43]. Notwithstanding, vibration characteristics at other locations along the structure are not indeed accounted for. This may cause problems if vibration reduction over the entire structure is needed. To deal with such issues, [29] have extended the  $H_2$  and  $H_\infty$  norms to spatially distributed systems. Before introducing the spatial controller, we address first and briefly the general robust design framework.

### 4.1 Modal model

Second-order differential modal equations are commonly used to represent structure behavior, because it is basic for a FE model, and can be easily converted to state-space formulation used in control area. Beginning with the nodal second-order approach, the concentrated parameters matrix equation of a generic mechanical structure is modelled as

$$M_p \ddot{p} + D_p \dot{p} + K_p p = B_0 F_a \quad (1)$$

where  $p$  is the displacement vector for the adopted nodes,  $M_p$ ,  $D_p$  and  $K_p$  are respectively the inertial, damping and stiffness matrices,  $F_a$  is the vector of external forces acting on the structure and  $B_0$  reflects its position distribution. Mechanical structures have an infinite number of vibration modes, and modelling them inevitably limits it to an adequate number, in order to represent the problem at hand. The modal matrix is defined as

$$\Phi = [\phi_1 \ \phi_2 \ \dots \ \phi_m]$$

where  $\phi_i$ ,  $i = 1, \dots, m$  are the first  $m$  natural modes. Considering the transformation for modal coordinates obtained using  $p = \Phi q$  and pre-multiplying (1) by  $\Phi^T$ , it results

$$\Phi^T M_p \Phi \ddot{q} + \Phi^T D_p \Phi \dot{q} + \Phi^T K_p \Phi q = \Phi^T B_0 F_a \quad (2)$$

that may be written as

$$M_m \ddot{q} + D_m \dot{q} + K_m q = B_m F_a \quad (3)$$

where  $M_m = \Phi^T M_p \Phi$ ,  $D_m = \Phi^T D_p \Phi$ ,  $K_m = \Phi^T K_p \Phi$ ,  $B_m = \Phi^T B_0$ , commonly known as modal matrices, with  $M_m$  and  $K_m$  diagonal matrices. In order to get also a diagonal modal damping matrix, which is very convenient for the modal analysis, it is common to adopt the proportional form,  $D_p = \alpha M_p + \beta K_p$ , where  $\alpha$  and  $\beta \geq 0$ . This assumption gives rather approximate values considering that flexible structures have very small damping factors in general.

#### 4.2 State-space model

Starting from (2), it is usual to choose the modal matrix  $\Phi$  such as the modal mass matrix results an identity matrix, leading to (4), for each mode,

$$\ddot{q}_i + d_{m,i}\dot{q}_i + k_{m,i}q_i = b_{m,i}F_{a,i}, \quad (4)$$

where  $i = 1, 2, \dots, m$ , is the mode index,  $d_m$  and  $k_m$  are the damping and stiffness coefficients for the respective mode. Even if a finite number of modes are considered, a model reduction approach is yet necessary to get a manageable model. Consider for the moment this reduced number  $n < m$  as the number of modes to control explicitly.

Adopting the state vector definition  $x(t) = [q(t) \ \dot{q}(t)]^T$  corresponding to modal displacements and velocities, the respective state-space model derived from (4) may be written as

$$\begin{aligned} \dot{x}(t) &= Ax(t) + B_w w(t) + B_u u(t) \\ y(t) &= Cx(t) \end{aligned} \quad (5)$$

where the four piezoelectric transducers seen in Fig. 3 are being considered as one control input  $u(t)$  (*Piezo 1*), two measured outputs vector  $y(t)$  (*Piezo 2* and *Piezo 3*) and disturbance input (*Piezo 4*). The system matrix  $A$  has dimension  $2n \times 2n$ , and is given by

$$A = \begin{bmatrix} 0_{m \times m} & I_{m \times m} \\ K_m & D_m \end{bmatrix}$$

where  $D_m$  and  $K_m$  are the diagonal matrices obtained from (4) but limited to only  $n$  modes. Notice that the  $B$  and  $C$  matrices must reflect the position of the respective transducers. We are here neglecting a possible feedthrough term between inputs and outputs.

#### 4.3 Spatial $H_\infty$ controller design

It is convenient to represent the adopted structure, in order to design its active controller, by the general MIMO system framework seen in Fig. 5. There, it may be seen two blocks and four signals, respectively the structural plant and controller blocks and disturbance and control signal vectors input signals  $w(t)$  and  $u(t)$ , and the time and spatial dependent performance index vector  $z(r, t)$  and measured output vector  $y(t)$ .

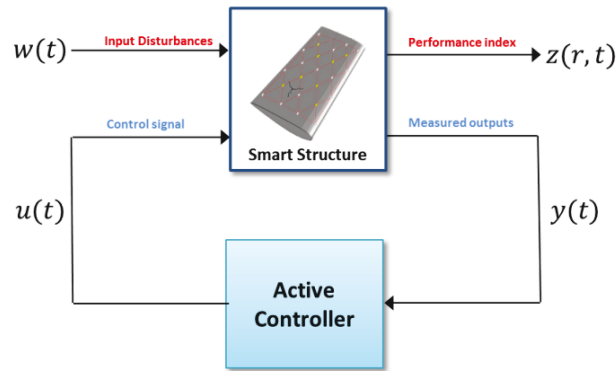


Fig. 5: Active control problem framework

In state space form, the plant to be controlled may be represented by (6), where  $x_p(t)$  is the state vector. All vectors and matrices must have adequate dimensions, regarding the number of inputs and outputs and the order of the plant. Considering the closed-loop system, its input is solely the disturbance vector and the performance vector is the output. In general, performance

index depends only on time. But to include the spatial restrictions we need to formulate the  $H_\infty$  spatial control problem where the performance output vector depends also on the spatial position. Considering initially only the time dependence, the state-space formulation is represented in (6):

$$\begin{aligned}\dot{x}_p(t) &= A_p x_p(t) + B_w w(t) + B_u u(t) \\ z(t) &= C_z x_p(t) + D_{zw} w(t) + D_{zu} u(t) \\ y(t) &= C_y x_p(t) + D_{yw} w(t)\end{aligned}\quad (6)$$

Given a state-space controller as

$$\begin{aligned}\dot{x}_k(t) &= A_k x_k(t) + B_k y(t) \\ u(t) &= C_k x_k(t) + D_k y(t)\end{aligned}\quad (7)$$

the  $H_\infty$  problem is to find the controller matrices which satisfy the infinity norm, stated as an optimization objective function for the transfer matrix  $T_{zw}$  between the disturbance  $w(t)$  and performance  $z(t)$  according to (6), which is a well-known problem.

$$J_\infty = \frac{\int_0^\infty z(t)^T z(t) dt}{\int_0^\infty w(t)^T w(t) dt} \quad (8)$$

To take into account a spatial region  $\Omega$  where we want to minimize the  $H_\infty$  spatial norm, a space dependent weighing matrix  $Q(r)$ , where  $r \in \Omega$  is the spatial vector, is introduced according to (9):

$$J_\infty = \frac{\int_0^\infty \int_\Omega z(t)^T Q(r) z(t) dr dt}{\int_0^\infty w(t)^T w(t) dt} \quad (9)$$

Considering the objective function in (9), the new performance vector may now be written as

$$z(r, t) = C_z(r) x_p(t) + D_{zw}(r) w(t) + D_{zu}(r) u(t) \quad (10)$$

or,

$$z(r, t) = [C_z(r) \quad D_{zw}(r) \quad D_{zu}(r)] [x_p(t) \quad w(t) \quad u(t)]^T \quad (11)$$

Defining an auxiliary matrix  $\Gamma$  such that

$$\Gamma^T \Gamma = \int_\Omega [C_z(r) \quad D_{zw}(r) \quad D_{zu}(r)]^T Q(r) [C_z(r) \quad D_{zw}(r) \quad D_{zu}(r)] dr \quad (12)$$

and the new performance index as

$$z_r(t) = \Gamma [x_p(t) \quad w(t) \quad u(t)]^T = [\Pi \quad \Theta_w \quad \Theta_u] [x_p(t) \quad w(t) \quad u(t)]^T,$$

it results

$$z_r(t) = \Pi x_p(t) + \Theta_w w(t) + \Theta_u u(t).$$

It is then possible to write the spatial objective function as

$$J_\infty = \frac{\int_0^\infty [x_p(t) \quad w(t) \quad u(t)]^T \Gamma^T \Gamma [x_p(t) \quad w(t) \quad u(t)]^T dt}{\int_0^\infty w(t)^T w(t) dt}, \quad (13)$$

conducting to (14), now similar to (8),

$$J_\infty = \frac{\int_0^\infty z_r(t)^T z_r(t) dt}{\int_0^\infty w(t)^T w(t) dt}. \quad (14)$$

which is similar to a regular  $H_\infty$  objective function. Then, the spatial  $H_\infty$  problem may be solved using known methods for the  $H_\infty$  problem.

#### 4.4 Model reduction

As mentioned before, real structures have an infinite number of vibration modes or degrees-of-freedom (DOF). To elaborate a useful mathematical model, we first choose an adequate number of nodes, which implies a consequent number of DOFs, reflecting a bandwidth of interest. To account for local geometrical details, especially to model damages and their spatial variations, FE method is the most used to model structures. FE method leads in general to significantly large models, impacting on the controller order, and eventually resulting in numerical difficulties. To solve this conflict, a model reduction technique is necessary.

The simplest approach for model reduction is by direct truncation, projecting the nodal displacements on a truncated modal matrix model. This pure truncation of high frequency modes is often a poor approximation. The neglected modes are ignored by assuming that their collective impact on the in-bandwidth modeled dynamics is minor. However, for control design purposes a controller based on such a model can alter zeros of the system, and, as closed-loop performances are largely dictated by open-loop zeros, one can expect differences between simulated and experimental results. It is, therefore, important to improve the reduced model of the system so that high performance controllers can be designed.

The approach used here is based upon including additional modes with resonant frequency far from the desired bandwidth, such that the flexibility of this single mode is equivalent to that of all out-of-bandwidth modes, omitted from the expansion. During the last decades, several publications have proposed to obtain a feedthrough term to capture the effect of truncated modes in an optimal way [25] [44]. In [29] and [30], the authors have extended this idea to the spatial model. In this case, the feedthrough term is found by minimizing the weighted  $H_\infty$  and  $H_2$  spatial norms of the error between the infinite dimensional and the truncated model [45]. However, from a FE simulation point of view, the modal basis with augmented states is generally preferred to using a feedthrough term. It induces only marginal increase of numerical cost.

In this work, given the position of actuators and sensors, the finite-dimensional model is obtained after a choice of a restricted subspace (or modes) that sufficiently describe the global dynamic behavior in the bandwidth of interest. Following the preceding discussion, the resulting reduced model is augmented by two second order poles, placed at least one decade beyond the bandwidth of interest. This model results in a system transfer function that maintains the appropriate pole-zero relationship.

## 5 SPATIAL $H_\infty$ CONTROL AND STRUCTURE DAMAGE

Next subsection presents details of the FE modeling of the healthy structure, for the complete and nominal models. In the sequence, the spatial  $H_\infty$  controller is designed and its performances are shown through comparison between structure response to disturbance and a controlled response. Finally, the last subsection shows the effect of a small damage on the structure response.

### 5.1 FE simulation of the healthy structure

Following the model reduction approach previously described, two second order out-of-bandwidth terms is included in the model, to ensure that the high frequency response content are close to that of the actual structure response. Damping value of  $\xi_i = 0.7$  and frequencies  $\omega_1 = 5000 \text{ rad/s}$  and  $\omega_2 = 5400 \text{ rad/s}$  were adopted for these two terms.

**Table 1:** Some natural frequencies of the healthy structure

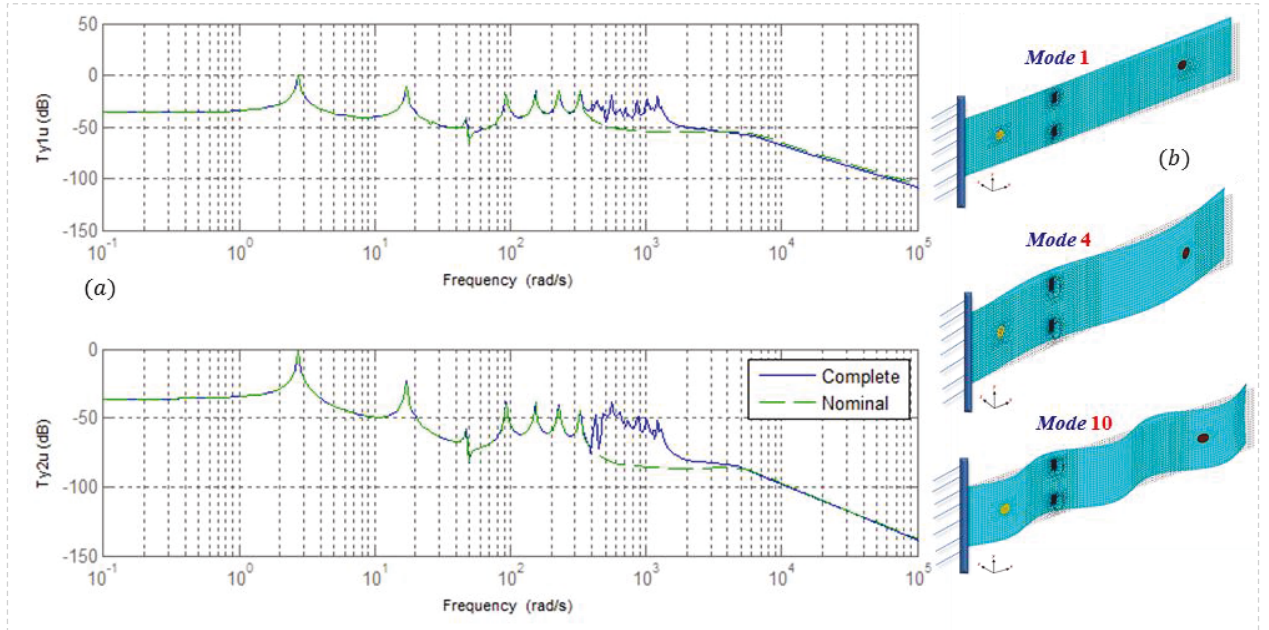
| Modes | Frequency (rad/s) | Modes | Frequency (rad/s) | Modes | Frequency (rad/s) | Modes | Frequency (rad/s) | Modes | Frequency (rad/s) |
|-------|-------------------|-------|-------------------|-------|-------------------|-------|-------------------|-------|-------------------|
| 1     | 2.7               | 6     | 93.3              | 11    | 278.2             | 16    | 448.0             | 22    | 742.2             |
| 2     | 16.9              | 7     | 140.2             | 12    | 325.5             | 17    | 475.9             | 25    | 742.2             |
| 3     | 26.6              | 8     | 152.7             | 13    | 366.5             | 18    | 493.1             | 30    | 1011.5            |
| 4     | 47.2              | 9     | 208.9             | 14    | 405.4             | 19    | 556.8             | 35    | 1184.1            |
| 5     | 79.5              | 10    | 228.3             | 15    | 430.7             | 20    | 564.3             | 40    | 1297.8            |

Two models are adopted for the numerical simulation: for the first one, which is used to design the controllers, only the 12 first modes are adopted, and it is here called the *nominal* model; and the second one, which is based on the first 40 modes and is used to simulate the performance of the designed controllers, we called the *complete* model. Fig. 6 shows the magnitude Bode diagram of the complete and the nominal transfer functions from the control input  $u$  to outputs  $y_1$  and  $y_2$ . Some natural frequencies are given in Table 1. Fig. 6 presents FE simulations including the piezoelectric patches and responses to modes 1, 4 and 10.

It may be seen Fig. 6a that the natural frequencies of the reduced nominal model, with the additional two frequencies, coincide with the complete model in-bandwidth low frequencies, and also the effect for additional modes in the high frequency response. It is to be also noticed that, depending on the considered input output path, some modes are not excited and so do not appear in the respective frequency response.

## 5.2 The spatial $H_\infty$ control of the healthy structure

The controller is designed to reduce the effect of the disturbance in a spatial  $H_\infty$  sense. The state space model for the nominal plant, including the spatial performance output is written as

**Fig. 6:** (a) Bode diagram of the complete and the nominal model; (b) Mode shapes 1, 4 and 10.

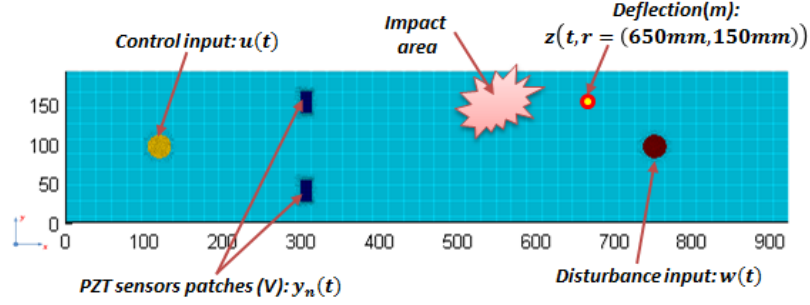


Fig. 7: Selected outputs, inputs and the impact zone to be monitored

$$\begin{cases} \dot{x}_n(t) &= A_n x_n(t) + B_{nw} w(t) + B_{nu} u(t) \\ z_n(t) &= \begin{pmatrix} \Pi \\ 0 \end{pmatrix} x_n(t) + \begin{pmatrix} 0 \\ R \end{pmatrix} u(t) \\ y_n(t) &= C_y x_n(t) \end{cases} \quad (15)$$

with  $R$  a weighting factor adjusting the level of the control signal, in order to have a satisfactory trade-off between control effort and vibration reduction, and  $\Gamma^T = [\Pi \ 0 \ 0]$  is obtained from the following integral

$$\Gamma^T \Gamma = \int_{\Omega} C_z(r)^T Q_w(r) C_z(r) dr$$

where the spatial weighting matrix  $Q_w(r)$  is chosen according to the region of the structure where we want to control the vibration.

Fig. 7 indicates the positions of the measured output vector  $y_n(t)$  and one arbitrarily chosen displacement output  $z(t)$ , which is only used to give a comparison reference of the controller performances. This performance output could be experimentally measured using a laser vibrometer. The respective controller, designed based on the healthy structure nominal model, is called here *the first controller*. The impact area, also indicated in Fig. 7, is the region where the subsequent damage will be included.

The first simulation refers to the healthy structure with unitary spatial weighting function, which means that the vibration reduction effort is equally performed along the plate. An adequate value of  $R$  is chosen ( $R = 0.3$ ) as a compromise between performance and stability. Fig. 9 shows the magnitude Bode diagram of the open loop and the closed loop system for the performance and the measured outputs. To highlight the controller effect on the vibration attenuation of the structure nominal modes we used in this case the nominal model to close the loop and obtain the frequency responses shown in Fig. 8.

For the next simulations, the controller is designed using the nominal plant model but we adopt the complete model to close the loop, in order to evaluate its robustness and spillover avoiding capabilities. The modes in Fig. 8a are numbered respecting the frequencies given in Table 1. Considering the  $z$  output, it is possible to notice that the peak reduction for mode 1 is more than 20 dB, what is true also for mode 2, with a smaller attenuation for modes 6, 8 and 10, and less attenuation at mode 4, near 5 dB. Modes 3, 5, 7 and 11 are not present in any response, open or closed loop. The  $y_1$  and  $y_2$  responses are similar to the  $z$  response.

Considering Fig. 9, where the complete model is used to close the loop, the in-bandwidth frequencies present the same behavior, and the highest frequencies did not show significant variation. We can notice that spillover is not present and this first controller shows good results.



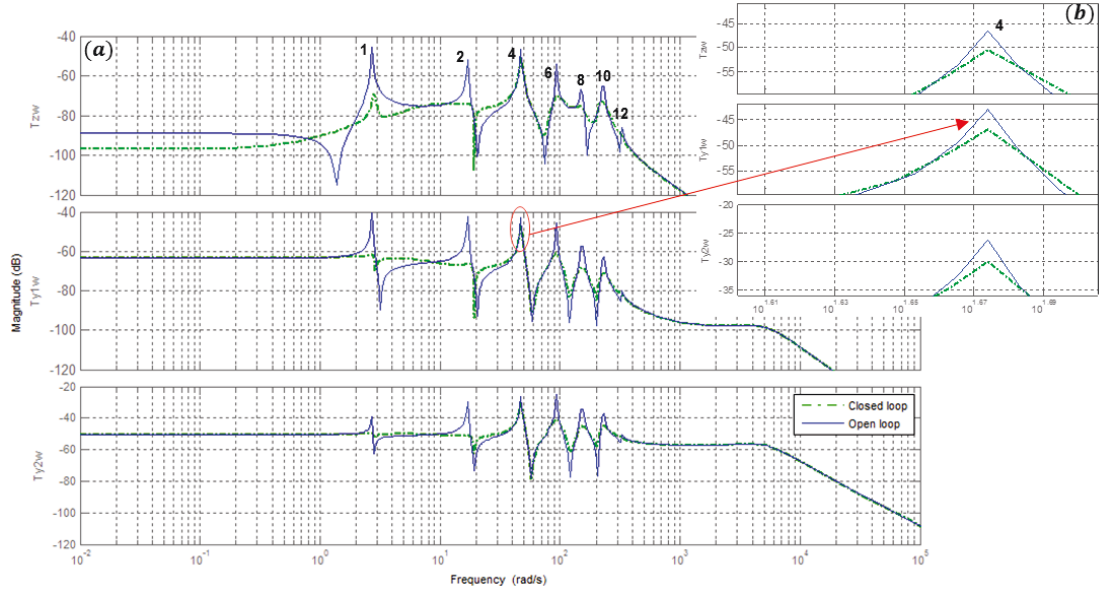


**Fig. 8:** (a) Bode diagram of the uncontrolled and controlled nominal structure. (b) Zoom on mode 4

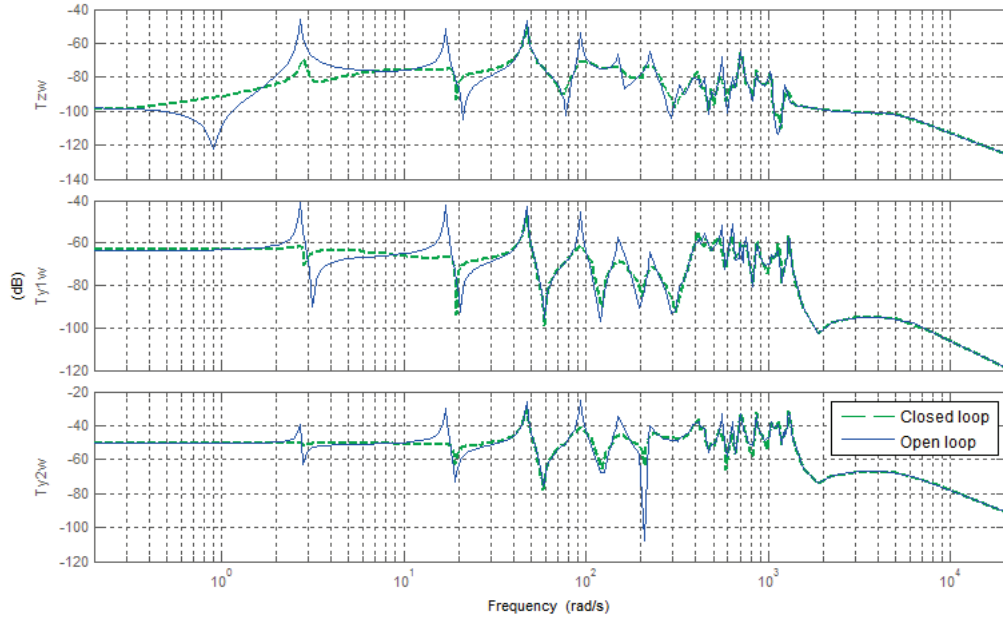


**Fig. 9:** Bode diagram of the uncontrolled and controlled healthy structure

The corresponding spatial frequency response of the system for the output  $y_1$  is presented in Fig. 10, where the third axis represents the position on the beam. These 3D diagrams permit to assess the controller spatial effect over the healthy structure. They show the simulated spatial frequency responses of the uncontrolled and the controlled structure. Here, we have taken the  $y$  position at its middle, *i.e.*  $y = 96 \text{ mm}$ , and measured the  $x$  along the structure while the frequency response (vertical axis) is in terms of the structure's transverse displacement. One should notice the mitigation of vibration of the entire structure, which has been also illustrated by the Bode regular diagram in Fig. 9.



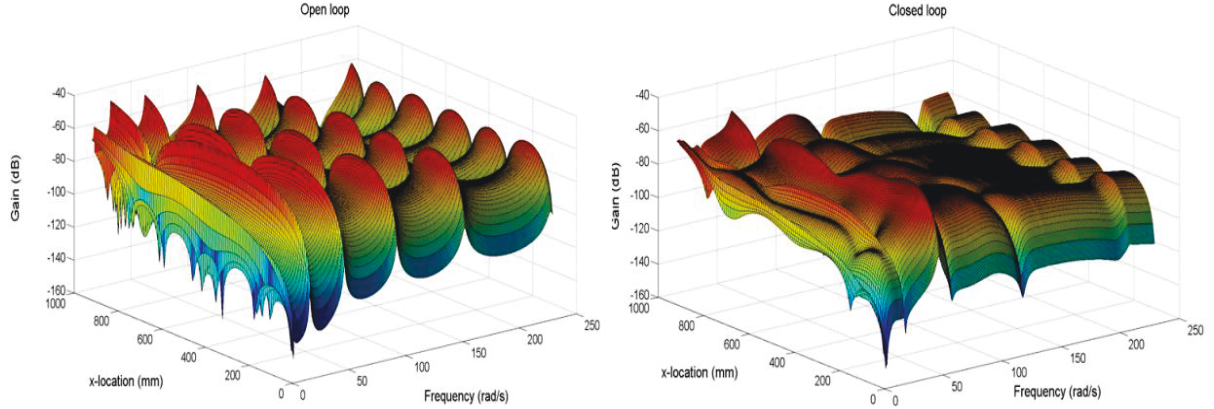


**Fig. 10:** Spatial transfer function response of the nominal system

Fig. 11 presents the  $H_\infty$  norm evaluated for the uncontrolled and controlled systems, in order to complement the analysis of the spatial effect of the controller over the healthy structure. It is clearly visible the effect of vibration reduction on the norm caused by the adopted spatial controller.

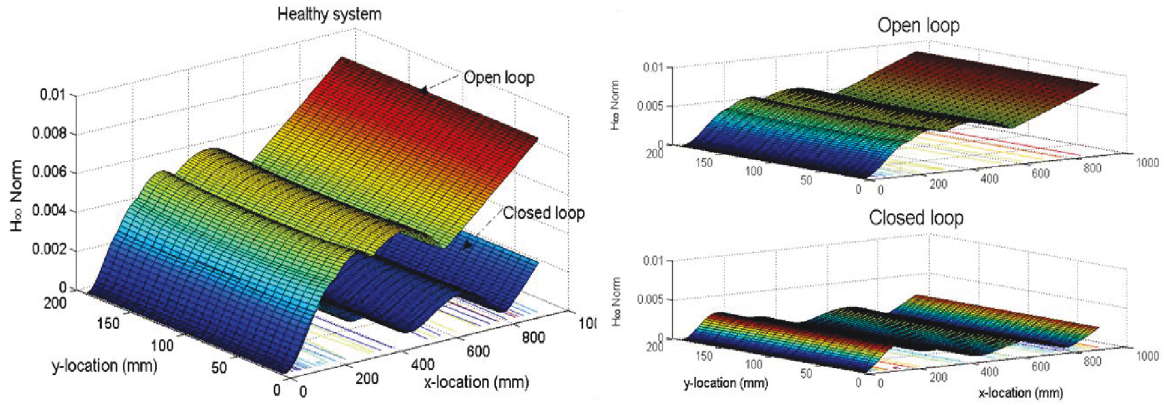


**Fig. 11:** Spatial  $H_\infty$  norm of the controlled and uncontrolled system ( $Q(r) = 1$ )

Time domain responses for both outputs for a Schroeder disturbance input signal can be seen in Fig. 12, for open and closed-loop, which complements the analysis of the system behaviour. The controller effectiveness can be easily assessed in these figures, considering the linear amplitude and also the linear sweep of the excitation signal from DC to 1570 rad/s in the shown 200 seconds period. It is visible also the attenuation in the in-bandwidth frequencies for the nominal model and that, for the extra frequencies of the complete model, the control signal increases or decrease the peak amplitudes by a small factor, but maintains the stability of the system.

### 5.3 Including damage

In this section we consider the effect of a barely visible impact damage (BVID), admitting  $\mathbf{Y} = 2 \times 10^{-3}$ , on the plant dynamics. Damage is represented, as described before, by a circular patch with diameter  $\varnothing = 20 \text{ mm}$ , centered at position  $(570, 140) \text{ mm}$  (see Fig. 13b). Fig. 13a illustrates the amplitude response of the complete model of the structure after including this damage. It is possible to see that the damage consequences on the plant model are small.

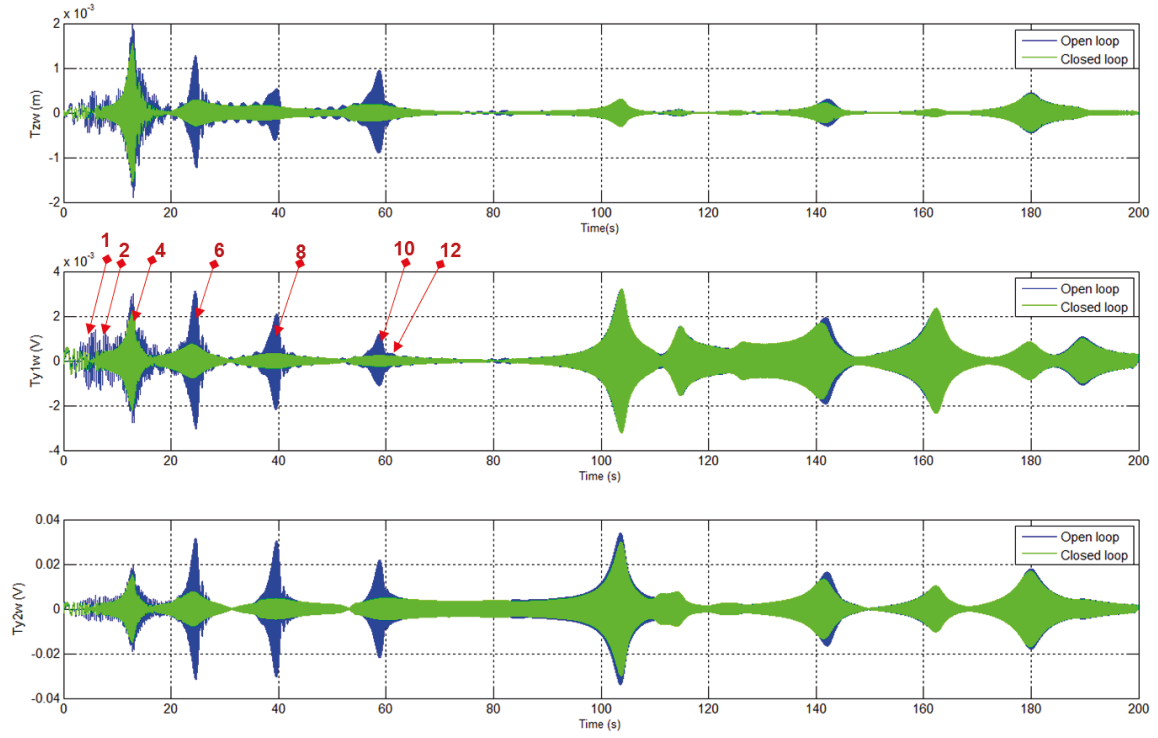


**Fig. 12:** Schroeder disturbance signal output responses of the healthy structure

Different response effects may result from different damages, which depend on several factors. It is possible for instance that the damage can lead to a decrease in the structure vibration on some regions. However, for the problem at hand, and considering this increase in the vibration, we aim to address the several possible DTAC strategies, to analyze how to change the controller in order to get the better possible performance of the respective controller.

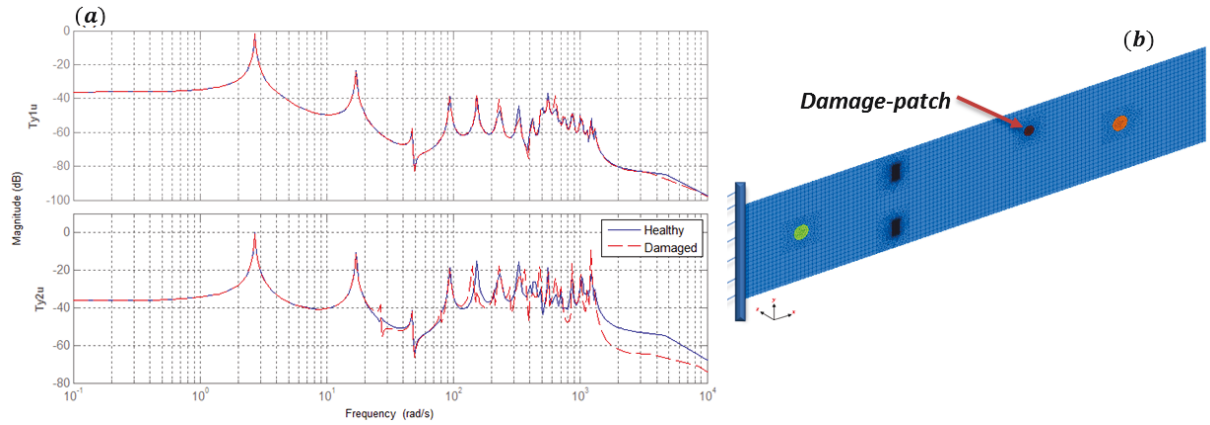


**Fig. 13:** (a) Comparing the effect on the complete model including a small damage. (b) BVID Damage centered at position  $(x = 570, y = 140) \text{ mm}$

## 6 APPLYING DTAC STRATEGIES

As mentioned before, there are several strategies to be adopted in a DTAC framework. For the present study, we are beginning in the next subsection with the basic approach where the controller is sufficiently robust to guarantee performance to some damage. In the sequence a controller reconfiguration scheme to accommodate the fault is presented and in the last subsection a controller to prevent evolution of damage is the subject, always based on  $H_\infty$  spatial control.

### 6.1 Robust active controller

The spatial  $H_\infty$  scheme has intrinsic robustness properties that can be straightforward used here to face small structural damages. Using the first  $H_\infty$  spatial controller, simulations of the healthy and the damaged systems are presented for the measured output vector,  $y_1(t)$ , and the spatial performance output  $z(t)$ . Fig. 14 shows the open-loop time response of the plane model to a Schroeder disturbance for the previous BVID damage, the closed-loop for the healthy plate response and the closed-loop where the first controller is being used after the occurrence of the damage.

Considering the damaged closed-loop response (Fig. 14) and comparing with the healthy closed-loop case, it is possible to notice a small increase in modes 4, 6 and 10, but a bigger increase in mode 8, both in the performance output and the measured output  $y_1$ . But, considering the open-loop response, there is yet attenuation due to the controller anyway. For the out-of-bandwidth frequencies, it is possible to notice amplification of the response, but also by a small factor.

Based on results in Fig. 14, showing that the differences between the healthy and the damaged closed-loop structure response are not significant, it is possible to conclude that a robust controller may deal with small damages. Obviously, this is a specific case, but it may be expected that similar results be achieved for several small level damages. Furthermore, if a damage study is performed first, the controller may then be designed to specifically reject the main damaging modes. That being said, the effect of a severe damage may not be so easily treated. In the following subsection, we study the effect of a severe damage on the closed loop responses.

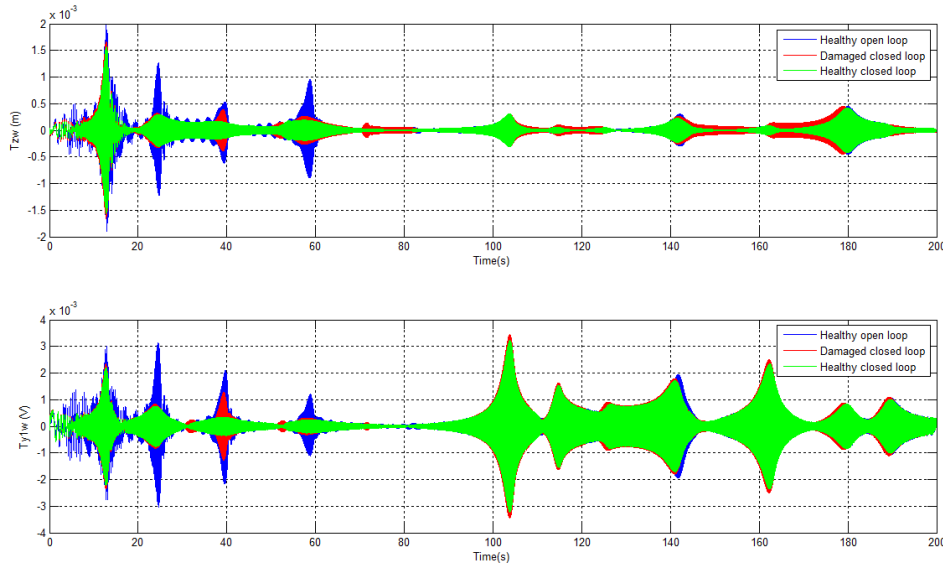


**Fig. 14:** Effect of a small damage on the first controller performance for a Schroeder disturbance response

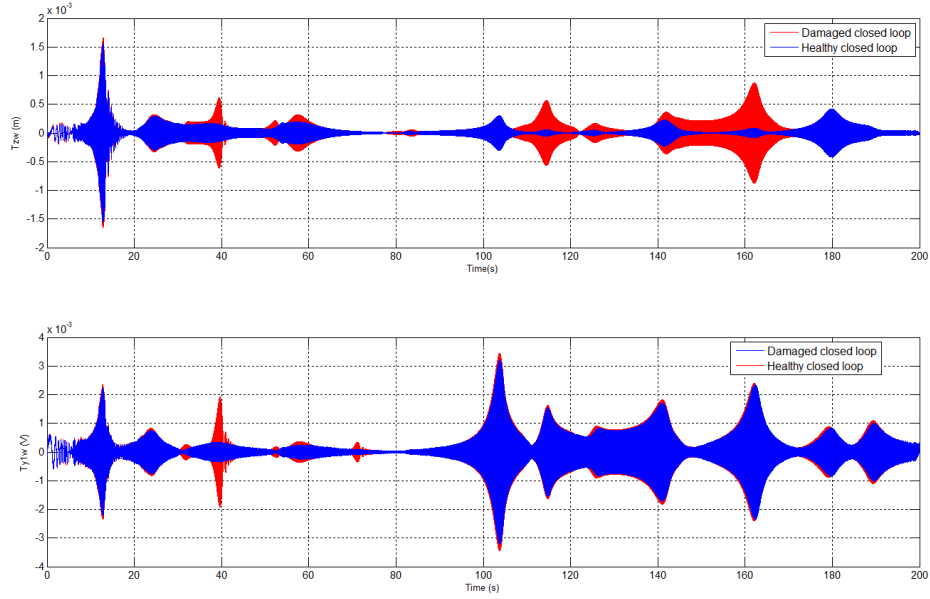


**Fig. 15:** Effect of a severe damage on the first controller performance

## 6.2 Reconfigurable Active Controller

The impact on closed-loop performance due to a severe damage may be much more significant than the previous case, conducting even to instability. Also, it may be expected that, for some *well-localized damage*, even if it is small, the consequence may be very significant. For these cases, an adaptive tolerance is required, demanding a DTAC strategy. A severe damage is considered here, adopting  $\mathbf{Y} = 2 \times 10^{-5}$ . Fig. 15 shows the effect of this damage on response to the same Schroeder disturbance input response, using yet the first controller.

It may be seen in Fig. 15 that now the first controller is not so effective. The performance output presents a significant increase in the level of several modes, and mainly in the higher frequencies. In the measured output, this is expected with the reduction of stiffness due to damage.

A reconfiguration to attenuate this damage effect is indicated, and in this case a new controller design needs to be conducted, which would be based on an experimental identification of the new structure. For an online redesign, this module is necessarily included in the framework, as described in Fig. 2. This reconfiguration module design demands some involved modeling and also a SHM method and we will be following here the simple approach. In the present case, a new controller was designed, based on the damaged FE model. Results for this new controller are shown in Fig. 16, where it is clearly visible how the new controller improves vibration mitigation, recovering a performance near to the one of the first controller. Fig. 17 presents  $H_\infty$  spatial norm distribution for the same simulation, and it is very useful to understand the reconfiguration controller effect.

In Fig. 17 it may be seen the previous three closed-loop systems. In the upper panel the healthy plate model with the first controller. In the middle panel, it may be seen the first controller facing the severe damage and in the lower panel, the second controller after reconfiguration. Damage effect in the plate under the strictly robust controller is clearly visible in Fig. 17b, showing high amplitude peaks located in the damage region. This effect is also seen in Fig. 17c, but the

respective peaks are here considerably attenuated, showing only a fraction of the energy from the previous case. It is implied that reconfiguration of the spatial controller achieved its goal, and we may expect that the operative life of the structure will be extended.

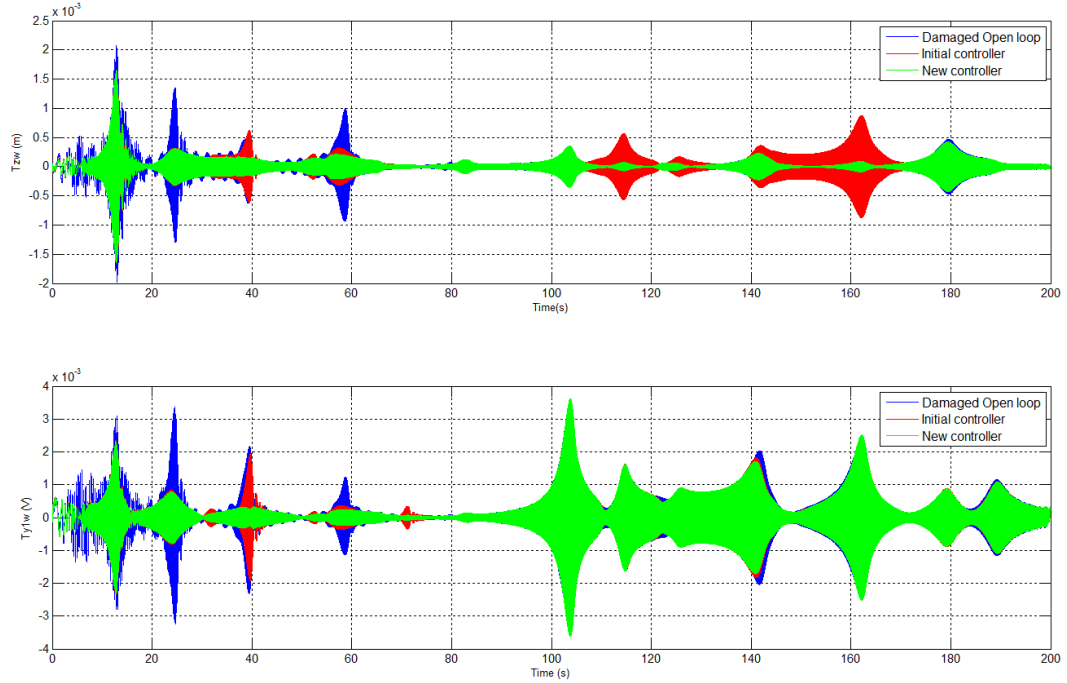


**Fig. 16:** Controller reconfiguration for a Schroeder disturbance

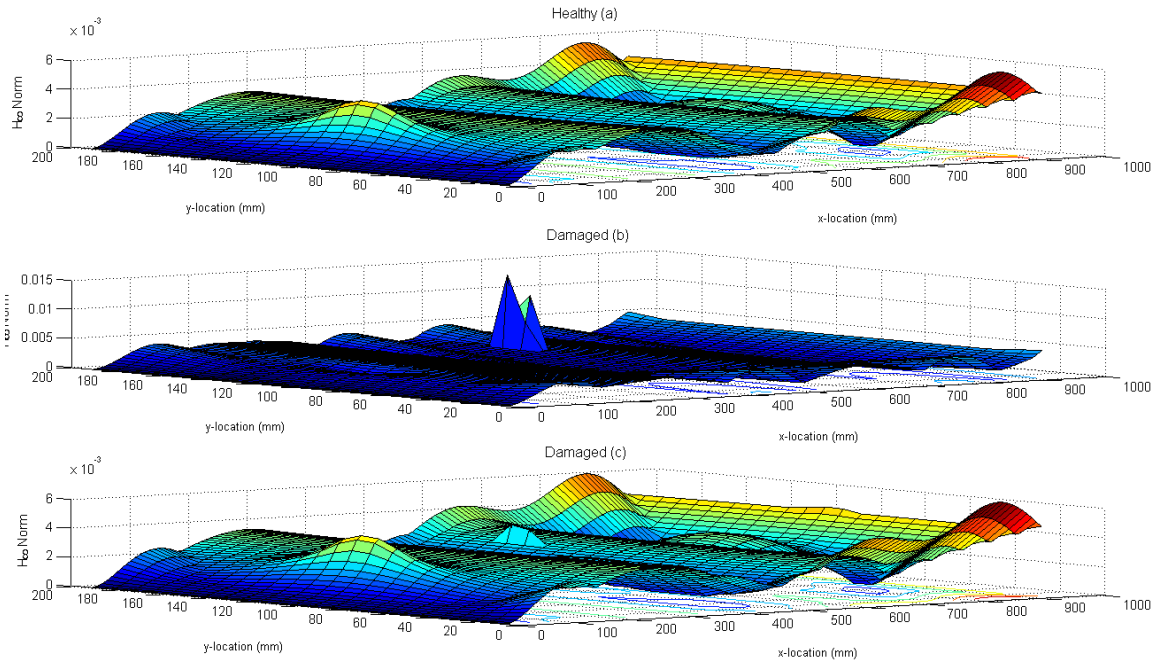


**Fig. 17:** Effect of a severe damage on the closed-loop  $H_\infty$  norm



### 6.3 Evolving active controller

The case where damage has been detected and localized, and we want to control its evolution, is addressed in this subsection, applying EDAC strategy. The idea is to try protecting the damaged area, in order to avoid the growth of the damage, attenuating vibration in the region where it is localized. This can be done by emphasizing the controller performance around the damaged area, albeit at the expense of vibration rejection performance over other regions. The spatial approach studied here is especially interesting to this strategy, providing this capacity through the spatial weighing function  $Q(r)$ . To show the effectiveness of the EDAC strategy, three weighing functions and a point-wise controller are simulated and their performances compared on assessing crack propagation.

A likely situation has been simulated by considering that the former severe damage has provoked crack propagation along one of the composite plies. Indeed, we have introduced a crack that begins from the border of the first impact damage to the border of the structure along the  $45^\circ$  direction of the ply. Thereby, a specific damage-patch has been added to the FE model with the impact damage, as shown in Fig. 18.

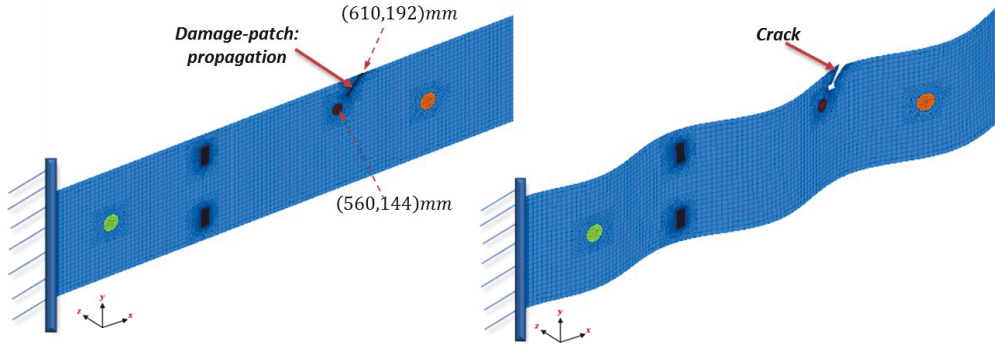


**Fig. 18:** Severe damage crack along the  $45^\circ$  direction

The crack measures  $68\text{ mm}$  and its effect on frequency response outputs are presented in Fig. 19. The changing due to this crack damage is easily seen as a significant one for the  $y_2$  response. We can also see in Fig. 20 how this crack affects the spatial  $H_\infty$  norm of the nominal system showing a big vibration increase, which could lead to instability.

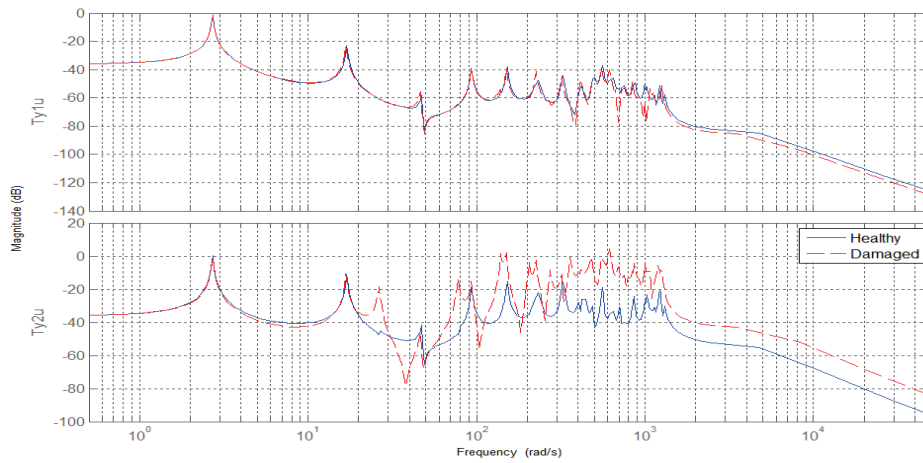


**Fig. 19:** Effect of crack damage on the frequency responses

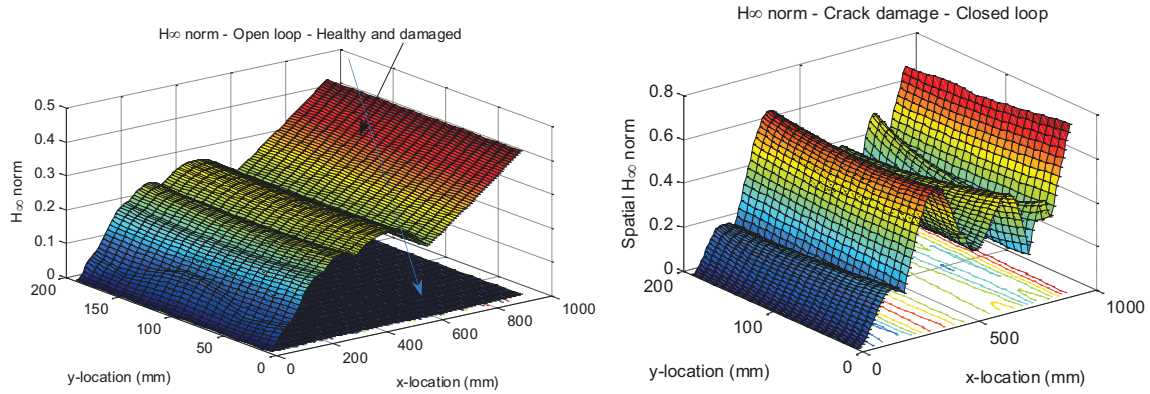


**Fig. 20:** Effect of the crack damage on the open and closed loop nominal system

Fig. 21 depicts the spatial adopted scheme, where the damaged area is depicted. Two different spatial weighing functions may be seen also in this figure, a Gaussian and a gate function, encompassing the regions where the damage is located. They are centered on a mid-point of the damage area with coordinates  $(570mm, 150mm)$ . The pointwise controller has been calculated for the position  $(650mm, 150mm)$ .

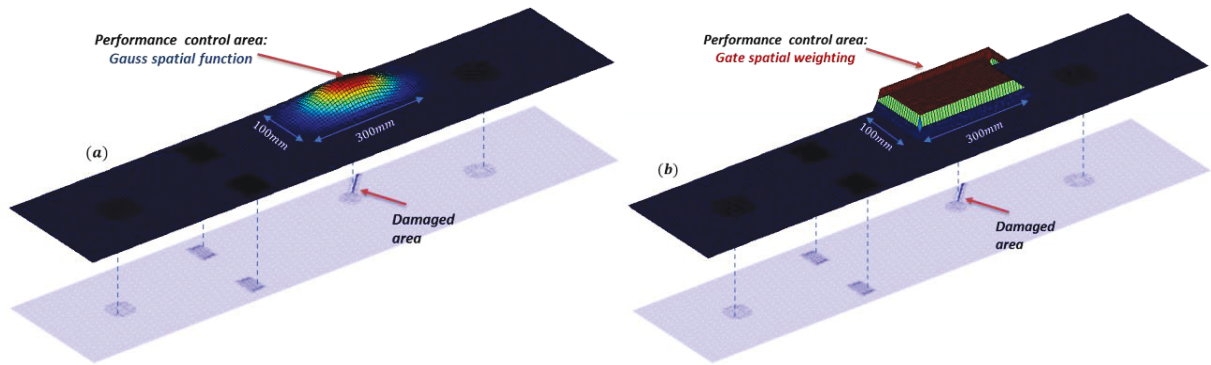


**Fig. 21:** Gauss (a) and Gate (b) spatial weighing functions  $Q(r)$

Fig. 22 presents results obtained for these two weighing functions, and also for a constant spatial weight for the complete beam, the pointwise  $H_\infty$  controller and the open-loop system, in terms of the  $H_\infty$  norm. It is possible to see that the open-loop  $H_\infty$  norm is growing along the  $x$ -axis, with an inflection due to the damage, and getting a high level after that. All controlled signals clearly show the attenuation in the vibration. To analyze these results, it is important to notice the region where damage is located and also the performance point used for the pointwise controller. The open loop response shows a minimum at the damage region, and then increases to the tip of the plate. The pointwise controller obtains the smaller norm, but only at the specific considered point, and after this point increases the norm in a rate bigger than the open loop system. At the region near the clamp of the plate the norm is similar to the others, but in the center it is higher. Considering the spatial controller with a constant weighing function, it presents a regular performance no the complete plate, and only in a region near the performance point the pointwise norm is smaller. Comparing this with the other two spatial function controllers, result of the constant weigh function controller is a little better in general, except in the region of the damage.

Considering that the objective here is to attenuate vibration on this region, the better one is the Gaussian weighing function controller, but both functions protect the damaged area, and the Gate function has a performance close to the Gaussian. It is possible to notice that the efficiency of the Gaussian weighing function is maximal around the center of the Gaussian.

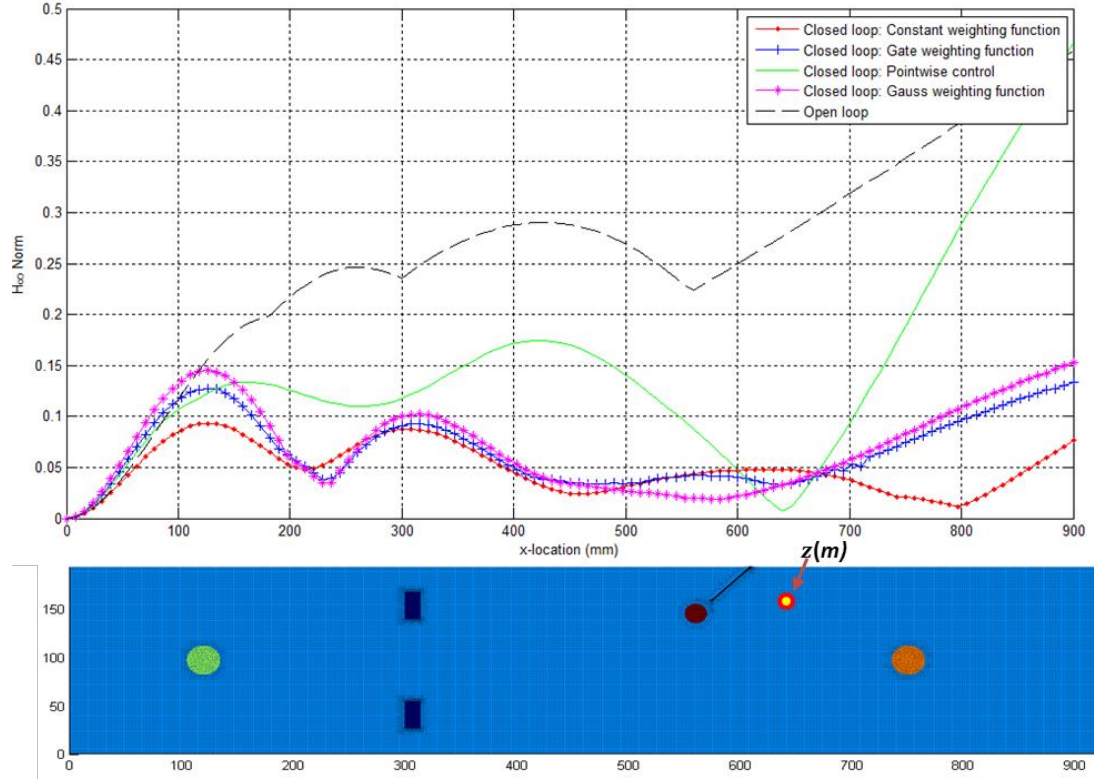


**Fig. 22:** Simulated closed loop spatial  $H_{\infty}$  norm for the nominal system as function of  $x$  at the line  $y = 150 \text{ mm}$

## 7 DISCUSSION

An investigation of the applicability of spatial  $H_{\infty}$  norm controller design to DTAC strategies was conducted here, through extensive FE modeling and simulations, including open loop and closed loop study of performance of several controllers and damage conditions, over a case study cantilever structure. Different controllers, corresponding to a different strategy were tested.

The first controller corresponds to the simple strategy to design a robust spatial  $H_{\infty}$  controller that may respond well to a structural damage. Results have shown that it is possible to expect that for small damages this may work with some loss of performance. Also, for a bigger damage, the loss of performance may be beyond an expected level, and it is possible to expect also that instability may come as a consequence of the damage localization, even though this did not occur in the simulations.

The second controller was designed according to the strategy that is supposed to become the most common, when a controller is reconfigured to attend a detected and localized damage. This control scheme may present a SHM module to provide these functions, and a reconfiguration



mechanism to use data so generated to change the controller parameters in order to face the damage. These two modules are necessary to guarantee an automatic online performance, and it is not treated here because goes beyond the scope of this paper. Also, it is possible to engage an engineer to provide the controller reconfiguration, what was adopted in this case. Results shown that it is possible to recover a good performance, similar to the original healthy controller, when the spatial  $H_\infty$  controller is used to face the damaged structure, under a severe damage.

Finally, the third analyzed strategy relates to the case when damage was detected and localized in some structure, and a controller is designed to maintain the respective damage region under low vibration, in order to guarantee an operative life extension to the structure. In this case, the spatial norm controller has shown specific features that confirm its vocation for DTAC application. Using four different optimization objectives, varying the spatial norm regions constraint, it was clearly shown the protection capacity of the controller over the known region of the damage, in this case corresponding to a Gaussian weighing function presenting the better performance.

It is possible to conclude also that the third strategy could be mixed with the first one, which becomes the second strategy presented in Fig. 1, the preventive active controller. Considering that we may know in advance the more probable region to show damage, the structure could be protected using an adequate weighing function, in order to prevent a future damage to occur, or at least retarding it.

## 8 CONCLUSIONS

This work aims to elaborate over some fundamental concepts and main strategies of DTAC application, presenting several  $H_\infty$  spatial norm controller design approach. Based on detailed FE models, developed to represent healthy and damaged structures, these controllers and strategies are assessed through various simulated results and diagrams.

Although FTC methods can be adapted to DTAC systems, peculiar characteristics of mechanical structures demands specific design solutions, which detach these two areas. In particular, spatial constraints, normally present on requirements of active control of structure vibration, indicate  $H_\infty$  spatial norm as a base for control design techniques of great interest for DTAC application. Those characteristics are illustrated on the analysis of the results here presented.

For the sake of completeness, mathematical modelling is briefly presented, from the structural control standing point. Simulated results of the addressed DTAC strategies exemplify the interesting properties of the spatial norm approach to face structural damage consequences.

As future development perspective, new methods to implement modules to provide online efficient reconfiguration and switching of controllers, and respective stability analysis, are under investigation. The mitigation of fatigue damage and how to take it into account in the design of the control algorithm are DTAC's topics that are also currently explored.

## APPENDIX

We present here the material properties of the active composite structure presented in Section 3.1. Hence, the materials properties of each composite layer of the structure are given in Table A1, whereas those of the two piezoelectric types in Table A2 and Table A3 respectively. The four piezoelectric patches were bonded using Epoxy glue (302-3M, produced by EPO-TEK) with properties given in Table A4.

**Table A1:** Mechanical properties of the composite material (23°C)

| Property | $\rho$<br>(g/m <sup>3</sup> ) | $E_{11} = E_{22}$<br>(GPa) | $E_{33}$<br>(GPa) | $\nu_{12}$ | $G_{12} = G_{13} = G_{23}$<br>(pC/N) |
|----------|-------------------------------|----------------------------|-------------------|------------|--------------------------------------|
| Value    | 1154                          | 69                         | 8.1               | 0,03       | 4.8                                  |

**TableA2:** Mechanical and electrical properties of the PZTs (NOLIAC®)

| Property | Dim<br>(mm)   | $\rho$<br>(Kg/m <sup>3</sup> ) | $E_{11}$<br>(GPa) | $E_{33}$<br>(GPa) | $\nu_{12}$ | $d_{31}$<br>(pC/N) | $d_{33}$<br>(pC/N) |
|----------|---------------|--------------------------------|-------------------|-------------------|------------|--------------------|--------------------|
| Value    | 28 × 14 × 0.1 | 7600                           | 62,50             | 52,63             | 0,38       | −195               | 460                |

**Table A3:** Mechanical and electrical properties of the MFCs (Smart Materials®)

| Property | Dim<br>(mm) | $\rho$<br>(Kg/m <sup>3</sup> ) | $E_{11}$<br>(GPa) | $G_{33}$<br>(GPa) | $\nu_{21}$ | $\nu_{12}$ | $d_{31}$<br>(pC/N) | $d_{33}$<br>(pC/N) |
|----------|-------------|--------------------------------|-------------------|-------------------|------------|------------|--------------------|--------------------|
| Value    | Ø30 × 0.1   | 5440                           | 30.4              | 5.52              | 0,16       | 0,38       | −170               | 400                |

**TableA4:** 302- 3M EPO-TEK glue properties

| Property | Operating<br>temperature | Coefficient of<br>thermal expansion   | Dielectric<br>constant | Dissipation factor | Storage modulus  |
|----------|--------------------------|---------------------------------------|------------------------|--------------------|------------------|
| Value    | − 55°C to 100 °C         | 193 10 <sup>−6</sup> °C <sup>−1</sup> | 3,39 at 1 kHz          | 0,0061 at 1 kHz    | 1,73 MPa at 23°C |

## REFERENCES

- [1] N. Mechbal and E.G.O. Nobrega, "Damage Tolerant Actice Control: Concept and State of Arts," in *Proceedings of the IFAC Conference on SAFEPROCESS*, Mexico, 2012.
- [2] R. Isermann, *Fault-diagnosis systems: An introduction from fault detection to fault tolerance*, Springer ed. Berlin , Germany, 2006.
- [3] M. Rébillat , R. Hajrya, and N. Mechbal, "Nonlinear structural damage detection based on cascade of Hammerstein models," *Mechanical Systems and Signal Processing*, vol. 48, pp. 247-259, 2014.
- [4] K. Worden, C. R. Farrar, G. Manson, and G., Park, "The fundamental axioms of structural health monitoring.," *Proceeding of the Royal Society*, vol. 463, pp. 1639-1664, 2007.
- [5] D. Balageas, C. P. Fritzen, and A. Güemes, *Structural Health Monitoring*. London: ISTE, 2006.
- [6] E. P. Carden and P. Fanning, "Vibration based Based Condition Monitoring: A Review," *Structural Health Monitoring Journal*, no. 3, 2004.
- [7] S.D. Fassois and J.S. Sakellariou, *Statistical Time Series Methods for SHM*, C. Boller and F. and Fujino, Y. Chang, Eds. Chichester, UK: John Wiley and Sons Ltd, 2009.
- [8] R. Hajrya and N. Mechbal, "Principal Component Analysis and Perturbation Theory Based Robust Damage Detection of Multifunctional Aircraft Structure," *Structural Health Monitoring an International Journal*, vol. 12, no. 3, pp. 263–277, 2013.
- [9] T. Massot, M. Guskov, C. Fendzi, M. Rebillat, and N. Mechbal, "Structural Health Monitoring Process for Aircraft Nacelle," in *ACMA'2014*, Marrackech, 2014.
- [10] D. J. Inman, C. R. Farrar, and V. Lopes Junior, *Damage Prognosis: For Aerospace, Civil and Mechanical Systems.*, 2005.
- [11] F.-K. Chang, "Structural Health Monitoring: Condition-based Maintenance," in *8th International*

*Workshop on Structural Health Monitoring (IWSHM)*, Stanford, 2011.

- [12] T.T. Soong, *Active Structural Control: Theory and Practice*. London: Longman Scientific, 1990.
- [13] A. Preumont, *Vibration Control of Active Structures, An Introduction*, second edition ed., Kluwer, Ed., 2002.
- [14] Rabih Alkhatib and M. F. Golnaraghi, "Articles Active Structural Vibration Control: A Review," *The Shock and Vibration Digest*, vol. 35, pp. 367-382, 2003.
- [15] B. Spencer and S. Nagarajaiah, "State of the Art of Structural Control," *Journal of Structural Engineering*, vol. 129, no. 7, pp. 845-856, 2003.
- [16] G. Cimellaro, T. Soong, and A. Reinhorn, "Integrated Design of Controlled Linear Structural Systems," *Journal of Structural Engineering*, vol. 135, no. 7, pp. 853-862, 2009.
- [17] J.O.M. Fernando, J.R. Arruda, and D.J. Inman, "Design of a reduced-order Hinf controller for smart structure satellite applications," *Philosophical Transactions of the Royal Society of London. Series A:Mathematical, Physical and Engineering Sciences*, vol. 359, no. 1788, pp. 2251-2269, 2001.
- [18] S.A. Frost and M.J. Balas, "Adaptive key component controllers for evolving systems," in *AIAA Guidance, Navigation, and Control Conference*, Honolulu, 2008.
- [19] R. Patton, "Fault tolerant control: the 1997 situation," , Hull, 1997, pp. 1033–1054.
- [20] M. Blanke, M. Kinnaert, J. Lunze, and M.. Staroswiecki, *Diagnosis and fault-tolerant control*, Springer ed. Berlin (Germany), 2006.
- [21] Y. Zhang and J. Jiang, "Bibliographical review on reconfigurable fault-tolerant control systems," *Annual Reviews in Control*, vol. 32, pp. 229–252, 2008.
- [22] P. Ambrosio, G. Cazzulani, F. Resta, and F. Ripamonti, "An optimal vibration control logic for minimising fatigue damage in flexible structures," *Journal of SoundandVibration*, no. 333, pp. 1269–1280, 2014.
- [23] B. Chomette, S. Chesné, D. Remond, and L. Gaudiller, "Damage reduction of on-board structures using piezoelectric components and active modal control – Application to a printed circuit board.," *Mechanical Systems and Signal Processing*, vol. 24, no. 2, pp. 352-354, 2010.
- [24] N. Mechbal, Vergé M., G. Coffignal, and Ganapathi, "Application of a Combined Active Control and Fault Detection Scheme to an Active Composite Flexible Structure," *International Journal of Mechatronics*, 2006.
- [25] S. O R Moheimani, H.R. Pota, and I.R. Petersen, "Spatial balanced model reduction for flexible structures," in *Proceedings of the American Control Conference*, vol. 5, 1997, pp. 3098-3102.
- [26] S.O.R. Moheimani, H.R. Pota, and I.R. Petersen, "Spatial control for active vibration control of piezoelectric laminates," in *Proceedings of the 37th IEEE Conference on Decision and Control*, vol. 4, 1998, pp. 4308-4313 vol.4.
- [27] S.O.R. Moheimani and T. Ryall, "Considerations on placement of piezoceramic actuators that are used in structural vibration control," in *Proceedings of the 38th IEEE Conference on Decision and Control*, vol. 2, 1999, pp. 1118-1123.
- [28] D. Halim and S. O R Moheimani, "Spatial resonant control of flexible structures-application to a piezoelectric laminate beam," *Control Systems Technology, IEEE Transactions on*, vol. 9, no. 1, pp. 37-53, 2001.
- [29] D. Halim and S. O R Moheimani, "Spatial H2 control of a piezoelectric laminate beam: experimental implementation," *Control Systems Technology, IEEE Transactions on*, vol. 10, no. 4,

pp. 533-546, 2002.

- [30] D. Halim and S. O. R. Moheimani, "Experimental Implementation of Spatial  $H_\infty$  Control on a Piezoelectric-Laminate Beam," *IEEE/ASME Transactions on Mechatronics*, vol. 7, pp. 346-356, 2002.
- [31] G. Barrault, D. Halim, C. Hansen, and A. Lenzi, "High frequency spatial vibration control for complex structures," *Applied Acoustics*, vol. 69, no. 11, pp. 933 – 944, 2008.
- [32] A.F. Mazoni, A.L. Serpa, and E.G.O. Nobrega, "A decentralized and spatial approach to the robust vibration control of structures," in *Challenges and Paradigms in Applied Robust Control*.: InTech Open Access Publishers, 2011, pp. 149-170.
- [33] M.A. Rastgaar, M. Ahmadian, and S.C. Southwar, "Orthogonal Eigenstructure Control with Non-collocated Actuators and Sensors," *Journal of Vibration and Control*, vol. 15, no. 7, pp. 1019–1047, 2009.
- [34] A.V. Srinivasan and D.M. McFarland, *Smart Structures: Analysis and Design*. Cambridge: University Press, 2001.
- [35] B. Chapuis, N. Terrien, D. Royer, and A. Déom, "Structural health monitoring of bonded composite patches using Lamb waves," in *Ultrasonic Wave Propagation in Non Homogeneous Media*, Proceedings in Physics Volume ed. Berlin: Springer, 2009, vol. 18, pp. 355-363.
- [36] M.A.O. Alves Jr., E.G.O. Nobrega, and T. Yoneyama, "Adaptive Neural Control for a Fault Tolerant System," in *7th IFAC Symposium on Fault Detection, Supervision and Safety of Technical Processes*, Barcelpna, 2009, pp. 137-142.
- [37] E. Balmes. (2012, December) Structural Dynamics Toolbox & FEM Link, User's Guide. [Online]. <http://www.sdtools.com/sdt/>
- [38] E. Balmes and A. Deramaecker, *Modeling structures with piezoelectric materials, Theory and SDT tutorial*. Paris: SDTools, 2013, <http://www.sdtools.com/help/piezo.pdf>.
- [39] C. Florens, E. Balmes, and F. Clero, "Test/Analysis comparison of piezoelectric patch local behavior for vibroacoustic active control application," in *Proc. of SPIE: Active and Passive Smart Structures and Integrated Systems*, 2007.
- [40] A. Benjeddou, "Piezoelectric smart structures and systems," *Smart Structures and Systems*, vol. 5, no. 6, p. Preface, 2009.
- [41] E. Balmes, M. Guskov, M. Rebillat, and N. Mechbal, "Effects of temperature on the impedance of piezoelectric actuators used for SHM," in *Vibrations SHocks and NOise*, Aix en provence, 2014.
- [42] S. Gopalakrishnan, M. Ruzzene, and S.V. Hanagud, *Computational techniques for structural health monitoring*. london: Springer Series in Reliability Engineering , 2011.
- [43] N. Mechbal, "Simulations and Experiments on Active Vibration Control of a Composite Beam with Integrated Piezoceramics.," in *17th IMACS World Congress*, Paris, 2005.
- [44] S.O.R. Moheimani and R.L. Clark, "Minimizing the truncation error in assumed modes models of structures," in *Proceedings of the American Control Conference*, vol. 4, 2000, pp. 2398-2402.
- [45] S.O.R. Moheimani and D. Halim, "A convex optimization approach to the mode acceleration problem," *Automatica*, vol. 40, no. 5, pp. 889-893, 2004.